From the cationic to the anionic alkali clusters: how the photoabsorption depends upon the total charge

Constantine Yannouleas
Department of Physics, Virginia Commonwealth University, P.O. Box 2000, Richmond, VA 23284, USA

Received 21 November 1991; in final form 6 March 1992

The evolution of the optical absorption spectra of alkali microclusters as a function of the total charge is studied using the random phase approximation upon a jellium background, while treating the Coulomb force in the local density approximation. For a specific number of delocalized electrons, the fragmentation of the oscillator strength increases, as one passes from the cationic to the anionic species. The cases of 8, 20, and 40 delocalized electrons are considered.

1. Introduction

The optical properties (i.e. the photoabsorption) of metal microclusters in the gas phase can be successfully investigated by beam-depletion spectroscopy. Indeed, several experimental measurements of photoabsorption cross sections have been carried out for a number of wavelengths and mass numbers (less than 40), and for a small number of different species. Specifically, concerning the pure clusters, measurements have been carried out for neutral sodium clusters [1–3], cationic potassium [4] and sodium [5] clusters, neutral cesium [6], and neutral lithium [7] clusters. Concerning the compound species, photoabsorption cross sections have been reported for cesium suboxide clusters [6], and for Li_xNa_y $(x+y=4)$ [7,8], Na_9Cl, and $ZnNa_8$ aggregates [9].

From the theoretical side, the optical behavior of metal clusters is most often interpreted within the framework of three approaches, namely, (1) the classical Mie-resonance theory for a metal sphere (ellipsoidal model) [2], (2) ab initio configuration-interaction molecular calculations that take into consideration the precise geometry of the ionic cores [10], and (3) microscopic methods based upon the jellium-background approximation, i.e. (i) the time-dependent local-density approximation (TDLDA) [11,12], (ii) methods that are closely related to the nuclear many-body problem (random phase approximation, RPA) [13–18] (for a description of the similarities between nuclear physics and metal cluster physics that provided the motivation for the development of the methods of this last category, cf. refs. [19–21]. In addition, ref. [22] has used an analytical approximation to the RPA polarization propagator in the coordinate space.

In particular, ref. [13] adapted the nuclear matrix-RPA to the case of spherical, closed-shell, homonuclear clusters. In this approach, the collective motion arises as a linear superposition over many single-particle transitions from the occupied to the *un*occupied orbitals of the effective average field that confines the delocalized valence electrons. For the spherical, neutral Na_{20} and Na_{40}, this method predicted multipeak photoabsorption profiles more complex than the simple one-peak profile expected [2] for the Mie theory [23] for the charge oscillations of a classical metal sphere. Such profiles have recently been observed experimentally [1,3]. They result from quantum size effects (interference effects) due to the discreteness of both the occupied and the *un*occupied single-particle levels. They are sensitive to the position of these levels, and thus to the corresponding effective potential that dictates the

Correspondence to: C. Yannouleas, Department of Physics, Virginia Commonwealth University, P.O. Box 2000, Richmond, VA 23284, USA.

detailed bunching of the orbital levels. Thus a fragmented optical response is another reflection of the electronic shell structure, inferred initially from the analysis of ground-state properties [24]. Fragmentation of the optical response has also been observed in the case of the neutral Cs_8 [6,25].

On the contrary, the cationic potassium clusters K_9^+ and K_{21}^+, with 8 and 20 valence electrons respectively, exhibit a one-peak profile [4], in good agreement with the ellipsoidal model [2] for the spherical clusters. As shown in earlier publications [13,26], this strikingly different behavior can be interpreted with the help of the matrix-RPA in a unified way, namely, as the effect of a strong modification of the effective potential of the cationic species, as compared to the neutral species. As will be discussed in this paper, the change in the effective potential modifies the shell structure and thus results in the observed variations of the photoabsorption profiles.

The present Letter extends the matrix-RPA calculations to the case of anionic alkali microclusters [#1], since ground-state properties of several of these species are already under experimental investigation [27]. In particular, starting from the changes in the effective potentials induced by the extra charges, the present Letter formulates a unified view of the global evolution of the optical response of pure metal clusters, as one passes from the cationic to the anionic species. In the following, the results of the matrix-RPA calculation will only be described, since the details of the formalism have been presented in previous publications [13,14] [#2].

2. RPA results and discussion

2.1. Variations in the effective potentials

Fig. 1 displays the LDA (local density approximation) effective potentials that bind the delocalized valence electrons in the case of the three species K_9^+, K_8 and K_7^-, namely for the cationic, neutral, and anionic potassium clusters, respectively, with eight delocalized electrons.

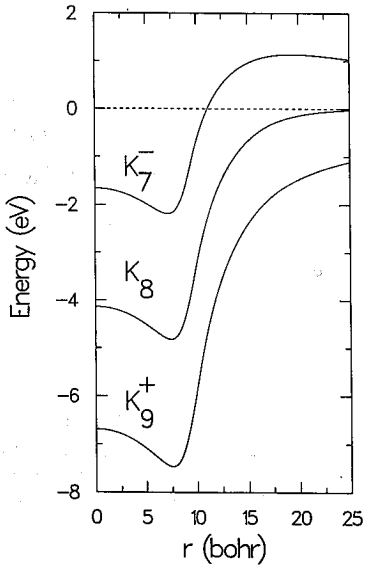

Fig. 1. Jellium potentials for K_9^+, K_8 and K_7^-.

The dramatic changes in the depth of these potentials are mainly due to the electrostatic contribution of the extra positive or negative charge. As was to be expected, the cationic potential is deeper compared to the neutral case, since the electrostatic attraction of the positive background upon the electronic cloud increases. The opposite is true for the anion.

Although modifications in the kinetic energy and in the exchange-correlation energy make a certain contribution, the change ΔU in the depth of the potential relative to the neutral case is roughly accounted for by the electrostatic potential generated at the origin by the extra charge $\pm\Delta Z$ assumed to be uniformly distributed over the volume of a spherical background of radius $R=r_sN_e^{1/3}$, namely

$$\Delta U=\mp\frac{3}{2}\frac{\Delta Ze^2}{r_sN_e^{1/3}}.$$

It follows that the difference from the neutral potential decreases as $N_e^{-1/3}$ with increasing electron number N_e. It is also interesting to notice that, the smaller the Wigner–Seitz radius r_s of the species under consideration, the larger its effect upon the po-

[#1] Since the particle–hole shell structure of small finite clusters is a priori taken into account by the matrix RPA, this method is most appropriate for describing the fragmented line shapes predicted below.

[#2] Other simpler RPA methods, like the semiclassical sum-rule techniques of refs. [15–17] or the analytical approach of ref. [22], owe their simplicity precisely in neglecting, or in oversimplifying, this shell structure, and thus are not the most advantageous for describing the complexity of the photoabsorption profiles.

tential depth is. Finally, it should be noticed that the anion develops a positive potential barrier. This can be understood by recalling that the LDA effective field is the potential seen by a small element of the electronic density due to the total number N_e of the delocalized electrons in the cluster.

2.2. Oscillator strengths and Thomas–Reiche–Kuhn sum rule

The RPA results described in section 2.3 were produced following closely refs. [13,14]. In particular, the single-particle energies and radial wavefunctions that enter into the RPA equations were specified by diagonalizing the single-particle Hamiltonians (sum of the kinetic term and of the effective potential) in a basis including 25 harmonic-oscillator major shells. The optimal oscillator parameter for this basis assumes the value of the major shell of a harmonic oscillator occupying the same volume as the neutral cluster. Due to the spherical symmetry, the single-particle energies ϵ_{nl} corresponding to the various effective potentials are characterized by only two indices, namely n and l, where n denotes the number of nodes plus one and l denotes the angular momentum.

The dipole transition probabilities associated with the RPA excited states $|n\rangle$ can be written as

$$B(E1, 0\rightarrow n)=\tfrac{2}{3}|\langle n\|\mathcal{M}(E1)\|0\rangle|^2, \qquad (1)$$

where $\langle n\|\mathcal{M}(E1)\|0\rangle$ are reduced matrix elements (cf. ref. [13,14]) of the dipole operator $\mathcal{M}(E1;\mu)=\sqrt{4\pi/3}\, er\mathcal{Y}_{1\mu}(\hat{r})$.

Since the RPA preserves the energy-weighted (Thomas–Reiche–Kuhn) sum rule $S(E1)=N_e\hbar^2e^2/2m$, the dipole transition probabilities (1) and associated RPA eigenenergies E_n obey the relation

$$\sum_n f_n=1, \qquad (2)$$

where the oscillator strengths f_n per delocalized electron are defined as

$$f_n=\frac{E_n\, B(E1, 0\rightarrow n)}{S(E1)}.$$

This result is also valid for the unperturbed excitations from an occupied to an unoccupied single-particle orbital (particle–hole transitions $|\mathrm{ph}\rangle$), that is

$$\sum_{\mathrm{ph}}(\epsilon_{n_p,l_p}-\epsilon_{n_h,l_h})\,|\sqrt{2/3}\,\langle \mathrm{p}\|\mathcal{M}(E1)\|\mathrm{h}\rangle|^2=S(E1).$$

Experimentally, the measured quantity is the photoabsorption cross section. To calculate the photoabsorption cross section σ per delocalized electron, one folds the RPA oscillator strengths with Lorentzian shapes normalized to unity as follows:

$$\sigma(E)=1.0975(\mathrm{eV\,\AA^2})\sum_n f_n\, L(E; E_n, \Gamma_n),$$

where Γ_n denotes the width of the Lorentzian profiles.

Since no measurements of cross sections for anionic clusters have been reported until now, the comparison with the neutral and positive ions will be limited in the following to a comparison of the corresponding oscillator-strength distributions.

2.3. Variations in the optical response

Fig. 2 displays the distribution of the RPA oscillator strengths as a function of energy for the three species K_9^+, K_8 and K_7^-. The response of K_9^+ and K_8 is dominated by a single line, carrying 96% and 85% of the Thomas–Reiche–Kuhn sum rule at an energy of 2.34 and 2.2 eV, respectively. On the contrary, the response of the anion K_7^- is substantially fragmented

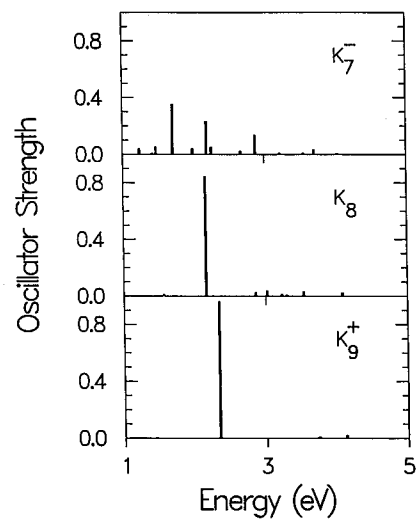

Fig. 2. RPA oscillator strengths for K_9^+, K_8 and K_7^-.

and spread out over a range from 1.2 to 3 eV. Even for the two similar cases of the cation and the neutral cluster, an increase in strength fragmentation is apparent as the total charge decreases. Concerning the position of the plasmon, a red-shift is noticeable as ΔZ decreases (ΔZ takes the values +1, 0 and −1 for the singly cationic, the neutral, and the singly anionic aggregates, respectively). Naturally, in the case of the anion, this observation refers to the average concentration of strength, since no single line can be interpreted as a collective plasmon.

The conspicuous variations of the optical strength from the cationic to the anionic species is directly related to the drastic changes induced in the effective potential by the extra charge (cf. fig. 1). Indeed, these changes modify the single-particle transitions from the occupied to the unoccupied orbitals (unperturbed particle–hole transitions), and thus they rearrange the extent of coupling between the collective motion (the plasmon) and the single-particle motion. Fig. 3 helps to form a visualization of this process, since it displays the distribution of the *unperturbed* oscillator strengths, namely, before the RPA diagonalization and the ensuing linear superposition are implemented upon the unperturbed particle–hole transitions. The scale of the vertical axis is logarithmic, so that the energies, $\epsilon_{n_p,l_p} - \epsilon_{n_h,l_h}$, of all relevant particle–hole transitions, that may participate in the linear superpositions determining the RPA states, can be directly traced. It should be noticed that most of the unperturbed strength resides with the particle–hole transitions of $\Delta N = 1$ character, where $N = 2(n-1)+l$ is the principal quantum number for the single-particle orbitals (in the figures, the $\Delta N = 1$ transitions are denoted with dashed bars).

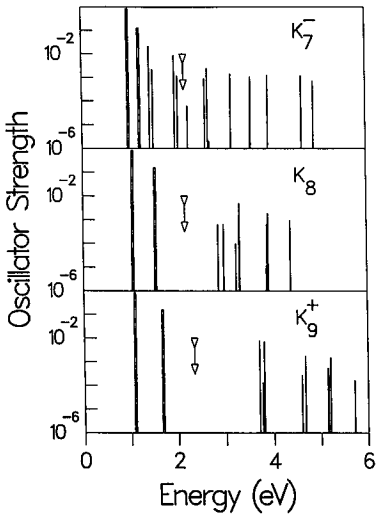

Fig. 3. The unperturbed particle–hole oscillator strengths for K_9^+, K_8, and K_7^-. The two particle–hole transitions of character $\Delta N = 1$ have the lowest energies and are denoted by dashed bars. The vertical arrow marks the position of the plasmon.

In the case of the unperturbed response of K_9^+, there is a large energy gap, $E_{G,ph}$, between the $\Delta N = 1$ transitions and the rest of the particle–hole transitions of character $\Delta N \neq 1$ (namely, $\Delta N = 3, 5, 7, \ldots$). As a result, the collective plasmon – whose position is marked by a vertical arrow – is built out in the RPA primarily from a superposition of the $\Delta N = 1$ transitions, and its energy falls well within the gap away from the $\Delta N \neq 1$ transitions. Thus the coupling between the plasmon and the $\Delta N \neq 1$ transitions is weak, and the RPA spectrum consists of one strong line. In general, for the aggregates considered in this Letter, the fragmentation of the RPA oscillator strength depends upon the extent of the coupling between the plasmon and the $\Delta N \neq 1$ unperturbed particle–hole transitions. Naturally, a larger distance between the vertical arrow and the forest of $\Delta N \neq 1$ transitions reflects a weakening of this coupling.

As seen from fig. 2, the case of the neutral K_8 is similar to that of the cationic K_9^+. However, in the neutral case, the energy gap $E_{G,ph}$ is smaller, and the vertical arrow lies closer to the edge of the $\Delta N \neq 1$ transitions (cf. fig. 3). Hence compared to K_9^+, the strength of the main RPA line for K_8 decreases by approximately 10%, while a high-energy tail develops comprising the same amount.

In the case of the anionic K_7^-, the gap between the $\Delta N = 1$ and the $\Delta N \neq 1$ transitions has practically disappeared. Thus the plasmon falls well inside the forest of the $\Delta N \neq 1$ transitions, and the resulting strong couplings yield a pronounced fragmentation of the RPA oscillator strength.

It should be noted that the position of the plasmon is rather insensitive to the changes in the effective potential, as one passes from the anionic to the cationic clusters. This is a consequence of the long-range character of the Coulomb force. On the contrary, the gap $E_{G,ph}$ immediately reflects these changes, and it

grows as the value ΔZ of the extra charge of the cluster varies from -1 to $+1$ (or $+2$). More precisely, the increase of the gap $E_{G,ph}$ reflects the weaker downward shifts in energy sustained by the *higher* unoccupied orbitals, as compared to the occupied orbitals, as well as to the *lowest* unoccupied ones. Indeed, as the potential becomes deeper, the higher unoccupied levels (namely, those that participate in the $\Delta N \geqslant 3$ transitions) are pulled downwards away from the rim of the potential and, eventually, they drop considerably inside the potential well. As a result, they are restricted to smaller volumes and, in accordance with the uncertainty principle, they acquire larger kinetic energies with regard to the previous step of a more shallow potential. On the contrary, the occupied orbitals are sufficiently well bounded, even in the anionic case, and their kinetic energies change relatively little following the downward movement of the potential bottom.

Another factor, that influences the value of this energy gap, is the size of the cluster. For the neutral clusters, the value of the gap decreases with increasing size resulting in variations of the photoabsorption profiles, as was described in detail in ref. [14] for the case of the magic Na_8, Na_{20}, and Na_{40}.

As figs. 4 and 5 show, the trend of increasing fragmentation of the optical strength with decreasing ΔZ is not limited to the case of eight delocalized electrons, but applies for larger sizes as well. In particular, fig. 4 describes the evolution of the optical response (RPA response) with decreasing ΔZ in the case of 20 delocalized electrons for potassium aggregates, while fig. 5 describes the corresponding evolution in the case of 40 delocalized electrons for sodium clusters. To further highlight this trend, fig. 5 exhibits in addition the case of the doubly charged N_{42}^{2+}. As was the case with fig. 3, figs. 6 and 7 help to provide a visualization of the fragmentation of the RPA optical response by displaying the corresponding unperturbed strength distributions and the evolution of the energy gap $E_{G,ph}$. Naturally, as was the case with eight delocalized electrons, the associated effective potentials in both the cases of 20 and 40 delocalized electrons become more shallow as ΔZ decreases.

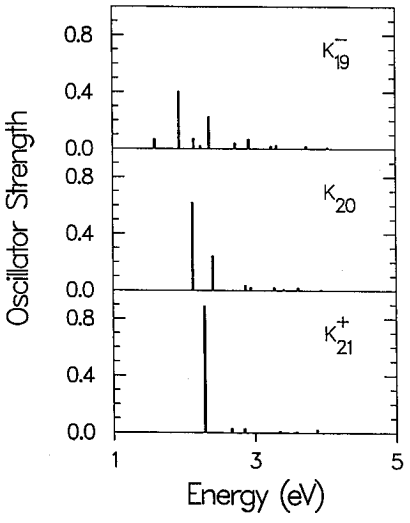

Fig. 4. RPA oscillator strengths for K_{21}^{+}, K_{20}, and K_{19}^{-}.

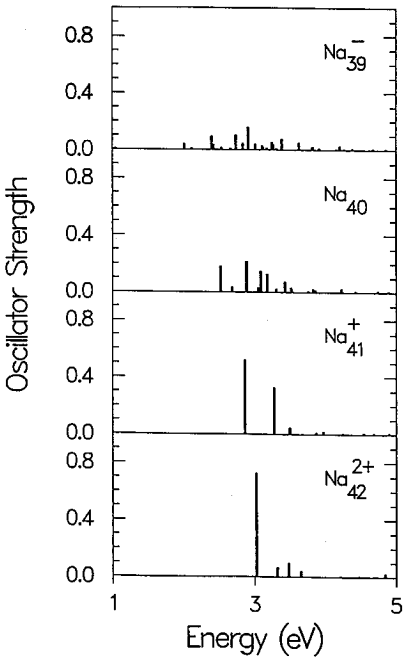

Fig. 5. RPA oscillator strengths for Na_{42}^{2+}, Na_{41}^{+}, Na_{40} and Na_{39}^{-}.

From fig. 5, one can see that, the larger the size of the cluster is, the larger the extra positive charge required for the disappearance of strength fragmentation. Indeed, a single strong RPA line appears in the case of the doubly charged Na_{42}^{2+}, but not in the case of the singly charged Na_{41}^{+}, unlike the cases of the singly charged K_{21}^{+} and K_9^{+} [#3].

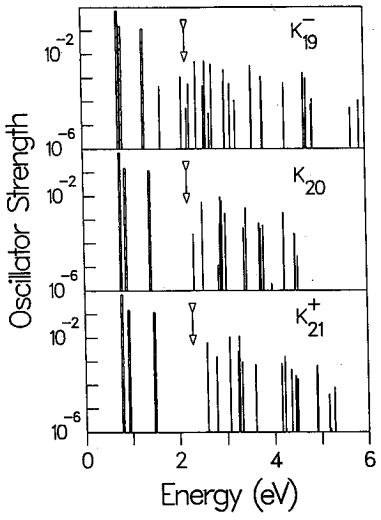

Fig. 6. The unperturbed particle–hole oscillator strengths for K_{21}^+, K_{20}, and K_{19}^-. The three particle–hole transitions of character $\Delta N=1$ have the lowest energies and are denoted by dashed bars. The vertical arrow marks the position of the plasmon.

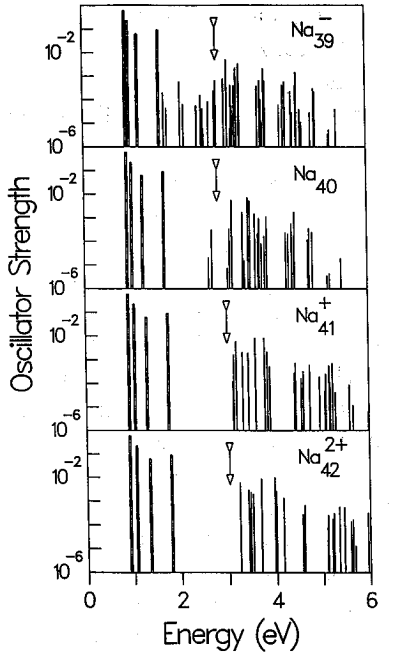

Fig. 7. The unperturbed particle–hole oscillator strengths for Na_{42}^{2+}, Na_{41}^+, Na_{40}, and Na_{39}^-. The four particle–hole transitions of character $\Delta N=1$ have the lowest energies and are denoted by dashed bars. The vertical arrow marks the position of the plasmon.

3. Comparison with the experiment and conclusion

Experimentally, photoabsorption cross sections have been measured only for a limited number of the clusters analyzed here. These are K_9^+, K_{21}^+ [4], and Na_{40} [1]. Additional measurements relevant to the present discussion have been reported for Na_8 and Na_{20} [1–3].

A detailed confrontation between the full matrix-RPA cross sections and the observations for the three neutral sodium clusters Na_8, Na_{20}, and Na_{40} was carried out in ref. [14]. It was found that, apart from a moderate blue-shift in energy, the present RPA theory was in good agreement with the experimental findings concerning the profiles and strength distribution. Moreover, the blue-shift in the position was found to decrease with the size, being only 5% for Na_{40}.

This blue-shift is systematic, and was found also in TDLDA calculations [11,12]. It is related to the fact that the LDA upon a uniform jellium background underestimates the static polarizabilities of small alkali clusters [24].

With respect to the cationic species, the blue-shift between the dominant RPA lines and those seen experimentally amounts to 10%–12% in the two cases of K_9^+ and K_{21}^+. Again, the agreement between RPA and experiment concerning the profiles and strengths is very good [#4]. It is thus natural to expect that, taking into consideration the moderate systematic correction in the position, the good agreement between the matrix-RPA results and experiment will extend also to the case of the anionic sodium and potassium species, as well as to the case of the cationic Na_{41}^+ and Na_{42}^{2+}.

In conclusion, the present Letter focused on the evolution of the optical response of spherical alkali

[#3] This statement should not been taken as implying that large metallic particles need to be strongly charged in order to display a single resonance line in their photoabsorption spectra (cross sections). Indeed, large metal clusters display the well-known, single-peak Mie resonance. In this case, the plasmon is highly fragmented, but the strength fragments bunch densely around the Mie energy. The impression of a single resonance line in the cross sections, exhibiting a width inverserly proportional to the radius of the cluster, arises from the envelop created by a very smooth fragmentation process (cf. in particular ref. [28], and references therein). Naturally, such a smooth fragmentation can arise only in the case of large clusters possessing quasi-continuum single-particle spectra.

For footnote 4 see next page.

clusters, as one passes from the cationic to the anionic species. The details of the RPA formalism (cf. refs. [13,14]) and of the corresponding numerical implementations were omitted in favor of a unified pictorial description of the factors that control this evolution. Such factors are the changes in the effective potentials that bind the delocalized electrons and the ensuing variations in the energy gap between the $\Delta N=1$ and $\Delta N>1$ *unperturbed* particle–hole transitions. For the smaller sizes of 8, 20, and 40 delocalized electrons, drastic reductions in the depth of the effective potentials develop with decreasing extra charge ΔZ. As a result, the fragmentation of the photoabsorption strength increases with decreasing ΔZ.

Acknowledgement

This work was supported in part by a grant from the US Department of Energy (DE-FG05-87ER45316).

[#4] Recently, the photoabsorption spectrum of Na_{21}^{+} has been reported in ref. [5]. The strength again is concentrated in a narrow energy region, much smaller than the case of the neutral Na_{20} (cf. ref. [3]), in accordance with the overall trend predicted by the matrix RPA [13]. However, the experimental cross section of Na_{21}^{+} is close to a Lorentzian shape exhibiting a narrow dip in the middle. The width of this dip is unusually small (≈ 0.05 eV) compared to the separation (≈ 0.3 eV) between the members of the double line in the neutral Na_{20}. Such a narrow dip may result from additional couplings outside the present RPA theory, namely, either from the two-particle two-hole additional shell structure accounted for in extensions of the RPA (second RPA, cf. ref. [29]), or from the neglected perturbation due to the geometrical arrangement of the ionic cores.

References

[1] K. Selby, V. Kresin, J. Masui, M. Vollmer, W.A. de Heer, A. Scheidemann and W.D. Knight, Phys. Rev. B 43 (1991) 4565.

[2] K. Selby, M. Vollmer, J. Masui, V. Kresin, W.A. de Heer and W.D. Knight, Phys. Rev. B 40 (1989) 5417;
W.A. de Heer, K. Selby, V. Kresin, J. Masui, M. Vollmer, A. Châtelain and W.D. Knight, Phys. Rev. Letters 59 (1987) 1805.

[3] S. Pollack, C.R.C. Wang and M.M. Kappes, J. Chem. Phys. 94 (1991) 2496;
C.R.C. Wang, S. Pollack, D. Cameron and M.M. Kappes, J. Chem. Phys. 93 (1990) 3787;
C.R.C. Wang, S. Pollack and M.M. Kappes, Chem. Phys. Letters 166 (1990) 26.

[4] C. Bréchignac, Ph. Cahuzac, F. Carlier and J. Leygnier, Chem. Phys. Letters 164 (1989) 433.

[5] C. Bréchignac, Ph. Cahuzac, F. Carlier, M. De Frutos and J. Leygnier, Z. Physik D 19 (1991) 1.

[6] H. Fallgren and T.P. Martin, Chem. Phys. Letters 168 (1990) 233.

[7] J. Blanc, M. Broyer, J. Chevaleyre, Ph. Dugourd, H. Kühling, P. Labastie, M. Ulbricht, J.P. Wolf and L. Wöste, Z. Physik D 19 (1991) 7.

[8] C.R.C. Wang, S. Pollack, J. Hunter, G. Alameddin, T. Hoover, D. Cameron, S. Liu and M.M. Kappes, Z. Physik D 19 (1991) 13.

[9] M.M. Kappes et al., to be published.

[10] V. Bonačić-Koutecký, P. Fantucci and J. Koutecký, Chem. Rev. 91 (1991) 1035; J. Chem. Phys. 93 (1990) 3802.

[11] W. Ekardt, Phys. Rev. B 31 (1985) 6360;
W. Ekardt and Z. Penzar, Phys. Rev. B 43 (1991) 1322.

[12] D.E. Beck, Phys. Rev. B 43 (1991) 7301.

[13] C. Yannouleas, R.A. Broglia, M. Brack and P.-F. Bortignon, Phys. Rev. Letters 63 (1989) 255.

[14] C. Yannouleas and R.A. Broglia, Phys. Rev. A 44 (1991) 5793.

[15] G. Bertsch and W. Ekardt, Phys. Rev. B 32 (1985) 7659.

[16] M. Brack, Phys. Rev. B 39 (1989) 3533.

[17] Ll. Serra, F. Garcias, M. Barranco, J. Navarro, C. Balbás and A. Mañanes, Phys. Rev. B 39 (1989) 8247.

[18] G.F. Bertsch, Comput. Phys. Commun. 60 (1990) 247.

[19] M.L. Cohen and W.D. Knight, Physics Today 43 (1990) 42.

[20] P. Jena, C. Yannouleas, S.N. Khanna and B.K. Rao, in: VII International Conference on Recent Progress in Many-Body Theories (Minneapolis, Minnesota, 26–31 August 1991), eds. C.E. Campbell and E. Krotscheck (Plenum Press, New York), in press.

[21] R.A. Broglia, J.M. Pacheco and C. Yannouleas, Phys. Rev. B 44 (1991) 5901.

[22] V. Kresin, Phys. Rev. B 40 (1989) 12507; Phys. Rev. B 39 (1989) 3042.

[23] G. Mie, Ann. Physik 25 (1908) 377.

[24] W.A. de Heer, W.D. Knight, M.Y. Chou and M.L. Cohen, Solid State Phys. 40 (1987) 93.

[25] C. Yannouleas and R.A. Broglia, Europhys. Letters 15 (1991) 843.

[26] C. Yannouleas, J.M. Pacheco and R.A. Broglia, Phys. Rev. B 41 (1990) 6088.

[27] K.M. McHugh, J.G. Eaton, G.H. Lee, H.W. Sarkas, L.H. Kidder, J.T. Snodgrass, M.R. Manaa and K.H. Bowen, J. Chem. Phys. 91 (1989) 3792.

[28] C. Yannouleas and R.A. Broglia, Landau damping and wall dissipation in large metal clusters, PREPRINT-NBI-91-36.

[29] C. Yannouleas, Phys. Rev. C 35 (1987) 1159;
C. Yannouleas, M. Dworzecka and J.J. Griffin, Nucl. Phys. A 397 (1983) 239.